Original Research

Enhancing volatile fatty acids production from waste activated sludge: The role of pretreatment by *N,N*-bis(carboxymethyl)-L-glutamate (GLDA)

Chang Liu [a], Lin Li [a,*], Linji Xu [a], Tanglong Zhang [a], Qiang He [a,**], Xiaodong Xin [b]

[a] *Key Laboratory of the Three Gorges Reservoir Region's Eco-environment, Ministry of Education, College of Environment and Ecology, Chongqing University, Chongqing, 400045, PR China*
[b] *Research Center for Eco-Environmental Engineering, Dongguan University of Technology, Dongguan, 523808, PR China*

ARTICLE INFO

ABSTRACT

N,N-bis(carboxymethyl)-L-glutamate (GLDA) is an eco-friendly chelating agent that effectively extracts multivalent metal ions from waste activated sludge (WAS) flocs, which could potentially alter their structure. However, the effect of GLDA on the production of volatile fatty acids (VFAs) from WAS is not well known. Here, we demonstrate that pretreatment with GLDA at a concentration of 200 mmol per kg VSS results in a significant increase of 142% in extractable extracellular polymeric substances and enhances the total VFAs yield by 64% compared to untreated samples. We reveal GLDA's capability to mobilize organic-binding multivalent metal ions within sludge flocs. Specifically, post-pretreatment analyses showed the release of 69.1 mg L^{-1} of Ca and 109.8 mg L^{-1} of Fe ions from the flocs, leading to a more relaxed floc structure and a reduced apparent activation energy (10.6 versus 20 kJ mol^{-1}) for WAS solubilization. Molecular dynamic simulations further demonstrate GLDA's preferential binding to Fe^{3+} and Ca^{2+} over Mg^{2+}. Our study suggests that GLDA pretreatment causes minimal disruption to reactor stability, thereby indicating the stability of microbial community composition. GLDA has emerged as a viable pretreatment agent for enhancing volatile fatty acids production from waste activated sludge.
© 2024 The Authors. Published by Elsevier B.V. on behalf of Chinese Society for Environmental Sciences, Harbin Institute of Technology, Chinese Research Academy of Environmental Sciences. This is an open access article under the CC BY-NC-ND license (http://creativecommons.org/licenses/by-nc-nd/4.0/).

1. Introduction

Waste activated sludge (WAS), a byproduct of the activated sludge process, has recently been produced in substantial quantities, necessitating proper attention [1,2]. The treatment and disposal of WAS represent a significant economic and environmental challenge, accounting for up to 60% of the total operation cost of wastewater treatment plants [3]. Characterized by high organic content in its solid phase, WAS serves as a potential substrate for anaerobic fermentation [4]. Volatile fatty acids (VFAs) are versatile intermediate products of anaerobic fermentation that could be used as carbon sources or precursors for value-added chemical commodities (e.g., polyhydroxyalkanoate, medium chain fatty acids) [5,6]. Therefore, VFAs production has attracted intensive attention as a promising technology to simultaneously stabilize and recover resources from WAS [7].

The solubilization and hydrolysis processes are commonly regarded as the rate-limiting steps of anaerobic fermentation owing to the stable semi-rigid structure of WAS flocs [7,8]. WAS comprises bacterial cells, extracellular polymeric substances (EPS), and other organic or inorganic components [9]. Among them, EPS is regarded as the backbone of WAS and is responsible for its stability [8]. The EPS structure can be strongly influenced by the multivalent metal ions (e.g., Ca^{2+}, Mg^{2+}, Fe^{3+}, etc.) [8,10]. For instance, Ca^{2+} can increase the floc mechanical stability by forming bridges with polyanionic alginate molecules of EPS [11]. Moreover, organic-binding metals constitute a significant fraction of the total measured metals presented in WAS [12,13]. They are reported to inhibit anaerobic digestion performance by increasing the thermodynamical barrier of sludge solubilization [8]. Hence, removing multivalent metal ions is expected to enhance VFAs production from WAS.

Many efforts have been devoted to improving anaerobic fermentation performance by removing the multivalent metals in

* Corresponding author.
** Corresponding author.
E-mail addresses: li.lin@cqu.edu.cn (L. Li), Hq0980@126.com (Q. He).

WAS [8,14]. Removing organic-binding metals with chelating agent EDTA (ethylene diamine tetraacetic acid) significantly enhanced the hydrolysis of WAS and increased the maximum VFAs production by 77% [8]. The isoelectric-point pretreatment could also release the multivalent metal ions from WAS matrix, resulting in 151.2% higher maximal VFAs production and 46.6% higher initial VFAs production rate [15]. However, this method necessitates using hazardous chemicals, such as HCl. Liu et al. [16] combined EDTA-2Na with protease pretreatment and obtained a final soluble chemical oxygen demand (SCOD) utilization rate of 0.93 mg VFAs per mg SCOD. Among these strategies, the chelating agent EDTA is widely used, specifically acting on metal ions [8,16,17]. However, EDTA is recalcitrant to biodegradation, which confers a high environmental persistence. Considering its excellent chelating ability, EDTA dramatically increases the risks of heavy metals leaching into aquatic or soil life [18,19]. Therefore, an efficient and environmentally friendly pretreatment technology is highly desired in this scenario.

N,N-bis(carboxymethyl)-ʟ-glutamate (GLDA) is an aminocarboxylate chelating agent which can be produced through a green chemistry process [20,21]. It exhibits excellent biodegradability and lower toxicity for organisms than traditional chelators like EDTA [22,23]. As a result, GLDA has been widely studied for heavy metals removal from soil [24], wastewater [22], and industrial sludge [21]. Hence, GLDA is expected to be able to remove multivalent metal ions in WAS and facilitate the anaerobic fermentation process without environmental concerns. However, there are limited studies on GLDA pretreatment on WAS [21,25]. To date, no information about multivalent metals removal from WAS by GLDA pretreatment and its mechanism for enhanced VFAs production is available. Therefore, it's crucial to reveal the pretreatment performances and its intrinsic mechanism.

This study investigated the effect and mechanism of GLDA pretreatment on VFAs production. The VFAs production performance was first determined. Then, organic matter release and the apparent activation energy for solubilization were explored. Variations in WAS physical properties and morphology induced by GLDA were also characterized. The multivalent metal ions fractions and molecular dynamic calculation between these metal ions and GLDA were conducted. Finally, the effects of GLDA on the microbial community stability were also investigated. The results of this study can promote the understanding of GLDA pretreatment technology, which may provide a new approach for enhanced resource recovery from WAS.

2. Materials and methods

2.1. Chemicals and WAS

GLDA-4Na (40%, $C_9H_9NNa_4O_8$, denoted as GLDA and used hereafter) was purchased in analytical grade from Aladdin company (Shanghai, China) and used as received. The WAS was obtained with a polypropylene container from a secondary sedimentation tank of a full-scale urban municipal wastewater treatment plant in Chongqing, China. This plant adopts the anaerobic-anoxic-oxic treatment process. The sludge was concentrated by settling at 4 °C for 24 h and stored at this temperature before use. The detailed characteristics of WAS are shown in Table 1.

2.2. Pretreatment and anaerobic fermentation

The pretreatment was conducted in six sets of serum bottles (18 bottles in total), each fed with 400 mL WAS. To each set of bottles, 0 (as control), 20, 50, 100, 150, and 200 mmol per kg volatile suspended solids (VSS) of GLDA were added, respectively. All bottles

Table 1
The main characteristics of sludge and inoculum used in this study.

Parameters	Raw sludge	Inoculum
TSS (mg L^{-1})	22.32 ± 0.42	42.58 ± 0.51
VSS (mg L^{-1})	9.99 ± 0.28	25.42 ± 0.36
SCOD (mg L^{-1})	333.56 ± 11.21	1571.09 ± 20.35
Soluble protein (mg COD L^{-1})	44.18 ± 0.80	85.34 ± 0.74
Soluble polysaccharide (mg COD L^{-1})	19.29 ± 0.39	35.54 ± 0.52
VFAs (mg COD L^{-1})	101.95 ± 2.67	1056.37 ± 16.73

were placed in a shaker (150 r min^{-1}, 25 °C) for 1 h. To study the effects of GLDA pretreatment on the acidogenic activity of WAS, the pretreated sludge was mixed with 10% inoculum obtained from an anaerobic fermentation reactor in the lab. The inoculum was centrifuged beforehand, and the supernatant was discarded to reduce its impact on the experiment; detailed characteristics are shown in Table 1. After that, 10 mmol L^{-1} 2-bromoethylsulfonate (2-BES) was added to inhibit disturbances from methanogenic activities [26]. All the serum bottles were flushed with nitrogen for 5 min to eliminate oxygen and capped with rubber stoppers. Then, put them into a water-bath shaker at 35 °C for 16 days. Liquid and gas phase samples were obtained regularly during fermentation to measure SCOD, soluble protein, soluble polysaccharide, VFAs, and the gas phase components.

2.3. Analytical methods

2.3.1. EPS extraction

After pretreatment, EPS was extracted by an improved centrifugal heating method to explore the effect of GLDA on EPS structures [27]. Briefly, 25 mL sludge suspension was centrifuged at 4000×g, and 4 °C for 5 min, and the supernatant was regarded as slime EPS (SL-EPS). The pellets were then resuspended to their original volume with 0.05 w/v% NaCl solution, which was preheated to 70 °C to ensure that the suspension temperature could reach 50 °C. Then, the suspension was immediately sheared with a vortex mixer (vortex Genie II, MO BIO Laboratories) for 1 min, followed by centrifugation at 4000×g and 4 °C for 10 min, and the supernatant was labeled as loosely-bound EPS (LB-EPS). The pellets were resuspended to the original volume again by 0.05 w/v% NaCl solution and incubated in a water bath at 60 °C for 30 min. The suspension was centrifuged at 4000×g and 4 °C for 15 min to obtain the supernatant as tightly-bound EPS (TB-EPS). The SL-EPS, LB-EPS, and TB-EPS were filtered through a 0.45 μm membrane before further analysis.

2.3.2. Imaging and morphology characterization of WAS

Confocal laser scanning microscopy (CLSM). CLSM (FV1200, Olympus, Japan) was employed to capture the images of the sludge samples before and after the pretreatment. SYTO 63 (Invitrogen, Carlsbad, USA), fluorescein isothiocyanate (FITC, Shanghai Yuanye Bio-Technology, China), concanavalin A (Con A, Xi'an Baiying Bio-Technology, China), and Calcofluor white (CW, Kulaibo Bio-Technology, China) were used to stain cells, proteins, α-ᴅ-glucopyranose polysaccharides, and β-D glucopyranose polysaccharides, respectively. Detailed operational procedures can be found in Text S1.

Scanning Electron Microscopy/Energy Dispersive X-ray Spectrometry (SEM-EDS). To observe the sludge morphology before and after the pretreatment, the samples were fixed with 2.50% glutaraldehyde solution for 2 h. Then, they were dehydrated with ethanol and *tert*-butyl alcohol. The samples were freeze-dried and then imaged with a scanning electron microscope (SEM, SEISS Gemini 300). The EDS spectrometer (OXFORD Xplore) was used for the

energy spectrum test.

2.3.3. Spectral determination of the organic matters

Excitation emission matrix (EEM) fluorescence spectra. A fluorescence spectrophotometer (F-7000, Hitachi, Japan) was used to obtain EEM spectra of the supernatant after the pretreatment. The obtained spectra could be divided into five groups according to the three-dimensional fluorescence regions (Table S1). The fluorescence regional integration (FRI) technique was utilized to calculate the fluorescent intensities of each region [28].

Fourier transform infrared (FTIR) spectroscopy. The WAS samples after GLDA pretreatment (0, 20, 50, 100, 150, and 200 mmol per kg VSS) were lyophilized. Around 1 mg of the freeze-dried sample was mixed with 200 mg of KBr to prepare the disc. The original and secondary derivative FTIR spectra were obtained at $4000-400$ cm^{-1} with an FTIR spectrometer (Nicolet iS20, Thermo Scientific, USA). Then, two-dimensional correlation spectroscopy (2D-COS) was adopted to improve the spectral resolution and characterize the change order of different functional groups of all the samples [9].

2.3.4. Thermogravimetric analysis (TGA) analysis

TGA analysis was conducted by a thermogravimetric analyzer (STA 449F5, Netzsch, Germany). Briefly, the samples were loaded and heated from 30 to 800 °C at a rate of 10 °C min^{-1} with an airflow rate of 50 mL min^{-1} under atmospheric pressure.

2.3.5. Metal fractionation analysis

After the pretreatment, the sludge sample was centrifuged at $5000 \times g$ for 10 min. The obtained supernatant was filtered through a 0.45 μm filter. Then, the soluble iron, calcium, and magnesium in the filtrate were measured by inductively coupled plasma atomic emission spectrometry (ICP-OES Agilent Technologies 5110, USA).

To examine the metal fraction in the solid phase, the sample was freeze-dried. The extraction method was adopted using the improved Tessier method (Table S2) [29]. Inductively coupled plasma mass spectrometry (ICP-MS Agilent Technologies 7800, USA) was used to determine the extracted metals. X-ray photoelectron spectroscopy (XPS) analysis of the freeze-dried sludge was carried out with an X-ray photoelectron spectrometer (ESCALAB 250Xi, Thermo Scientific, USA).

2.3.6. DNA extraction and high-throughput sequencing

The variations of the microbial communities during the experiment were explored using 16S rRNA gene high-throughput sequencing conducted by Majorbio Bio-pharm Technology Co., Ltd. (Shanghai, China). At the end of anaerobic fermentation, the slurry samples were collected on day 16. They were centrifugated at 10000 rpm for 10 min, and the pellet was stored in a sterile tube at −80 °C. The DNA was extracted according to E.Z.N.A® soil kit instructions (OMEGA soil DNA Kit, Omega Bio tek, USA). The ultramicro spectrophotometer (NanoDrop2000, Thermo Scientific, USA) was used to detect the concentration and purity of DNA. After quality determination by 1% agarose gel electrophoresis, the extracted DNA was amplified by polymerase chain reaction (PCR) with the universal bacterial primers 338F-806R (5′-ACTCC-TACGGGGAGGCAGCAG-3′, 5′-GGACTACNNGGGTATCTAAT-3′). The PCR products were used for the subsequent paired-end sequencing on an Illumina platform. The data obtained was analyzed on the online platform of Majorbio Cloud Platform (www.majorbio.com).

2.3.7. Other analytical methods

Total suspended solids (TSS), VSS, and SCOD were measured using standard methods [30]. The total organic carbon (TOC) was analyzed with a TOC analyzer (Shimadzu TOC-L CPH, Japan). The samples were filtered through 0.45 μm filters before measurement.

The soluble polysaccharide was determined by the anthrone sulfuric acid method, with glucose as the standard. The soluble protein was determined by the BCA protein determination kit (Beijing Suolaibao Technology Co., Ltd.). The COD conversion coefficients of polysaccharides and proteins were used according to a previous study [31]. CH$_4$, CO$_2$, N$_2$O, and VFAs were analyzed by gas chromatography during the fermentation (Techcomp GC7900, China). The COD conversion rates of acetic acid, propionic acid, isobutyric acid, *n*-butyric acid, isovaleric acid, and *n*-valeric acid are 1.07, 1.51, 1.82, 1.82, 2.04, and 2.04, respectively [32]. The capillary suction time (CST) and Zeta potential after the pretreatment were measured by a CST time meter (Hengomei HDFC-10A, China) and a Zeta potential analyzer (Malvern Zetasizer Nano ZS90, UK). The apparent activation energy (AAE) value of sludge was calculated with the Arrhenius equation (details in Text S2).

2.4. Molecular dynamic (MD) calculation

The molecular model of C$_9$H$_9$NNa$_4$O$_8$ and the chemical structure were downloaded from the PubChem website. All simulations were performed using the Focite module in Material Studio 2019 with the COMPSS force field [33]. The models were simulated for a total of 1 ns, with additional details on the computation and analysis of trajectories given in Text S3 and Text S4.

3. Results and discussion

3.1. Anaerobic fermentation performances

The anaerobic fermentation performance from WAS pretreated with different concentrations of GLDA was first evaluated. As shown in Fig. 1, all the SCOD, VFAs, proteins, and polysaccharides in the supernatant increased with a higher dosage of GLDA, implying a positive effect of GLDA pretreatment on the anaerobic fermentation process. The SCOD increased with the fermentation time and reached a plateau after day 10. The SCOD was around 3428 mg L^{-1} in the 200 mmol per kg VSS test, which increased around 78% of that in the control test (around 1929 mg L^{-1}). Clearly, the addition of GLDA improved the solubilization and hydrolysis efficacy of WAS.
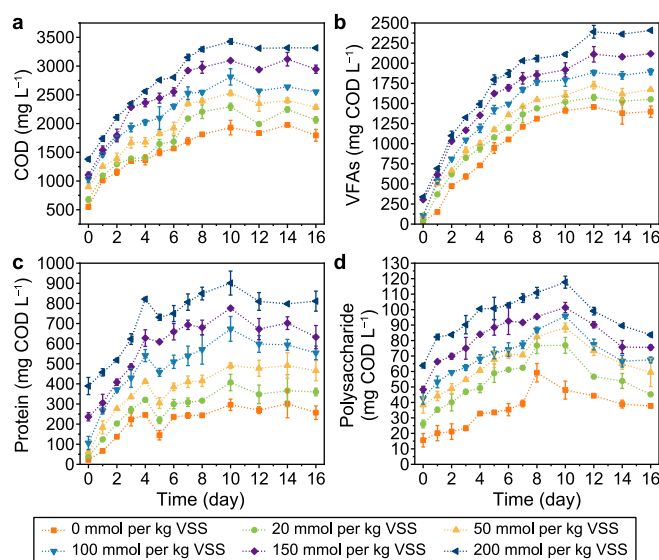

Fig. 1. Variations of soluble organic matter during anaerobic fermentation pretreated with different concentrations of GLDA: **a**, COD; **b**, VFAs; **c**, Protein; **d**, Polysaccharide. The error bar represented the standard error of the triplicate samples.

The VFAs displayed a similar tendency but increased and reached a plateau on day 12. The total VFAs was 2391 mg COD L^{-1} on this day in the 200 mmol per kg VSS test, which was about 64% higher than the control (1457 mg COD L^{-1}). This performance was similar to the VFAs production involving other pretreatments previously [34,35]. Apparently, the pretreatment significantly improved the VFAs production performance. Moreover, the SCOD achieved a plateau on day 10 while VFAs continually increased until day 12. Fig. 1c and d shows that both protein and polysaccharide reached their maximum values on day 10 and then decreased. It indicated that most of the available substrate for anaerobic fermentation was released from WAS on day 10, following the stable SCOD and VFAs concentrations afterward. As for the SCOD distribution, the VFAs proportion slightly decreased with higher GLDA dosages on day 12. The total VFAs accounted for 72% and 79% of the SCOD in the 200 mmol per kg VSS and control tests, respectively.

The distribution of individual VFAs is depicted in Fig. 2. As demonstrated, no significant impact on VFAs distribution by GLDA was observed. In all tests, acetate (over 50%) was the most abundant product, followed by propionate (over 15%) in the supernatant, which was consistent with the reported 50.64% (acetate) and 10.06% (propionate) in previous studies [7,36]. The proportion of acetate remained relatively stable under different pretreatment conditions. For instance, on day 12, the acetate accounted for approximately 55.7%, 55.8%, 52.4%, 51.8%, 54.4%, and 53.3% of the total VFAs with increasing dosages of GLDA, respectively. Meanwhile, the propionate proportions were 11.9%, 12.0%, 14.6%, 16.1%, 15.2%, and 17.1%, respectively. These results suggested that the propionate proportion slightly increased with the addition of GLDA, while the production of VFAs with longer carbon chains was reduced. In the gas phase, CO_2 was detected as the dominant product in all the tests during the anaerobic fermentation (Fig. S1). Clearly, GLDA pretreatment increased the CO_2 content in the gas phase, indicating high microbial activity induced by the pretreatment.

3.2. Organics solubilization from WAS

The solubilization of organic matter from WAS was then explored as it was regarded as the rate-limiting step [8]. Since EPS accounted for a large proportion of WAS, the EPS structure was studied subsequently. As shown in Fig. 3a, the soluble COD (i.e., SL-EPS), protein, and polysaccharide increased significantly with increasing dosages of GLDA during pretreatment. The total soluble organics were 108.2, 149.2, 190.2, 303.8, 384.3, and 534.1 mg COD L^{-1} with increasing GLDA dosages, respectively. However, the WAS

Fig. 2. Distribution of individual VFA during the anaerobic fermentation process. The individual column from left to right in the same day is corresponding to GLDA dosages of 0, 20, 50, 100, 150, and 200 mmol per kg VSS. The error bar represented the standard error of the triplicate samples.

solubilization was not outstanding compared to other pretreatments [16,37]. For example, thermal alkaline hydrolysis pretreatment could release as much as 19273.2 mg per L COD from WAS [16]. Considering that extractable EPS (other than SCOD) was more appropriate for evaluating the pretreatment performance, EPS structure was further analyzed after the pretreatment. EPS was mainly composed of polysaccharides and proteins (especially proteins) according to EPS structure analysis, also reported previously [38]. The total extracted EPS increased from 701.6 mg COD L^{-1} (control) to 1734.8 mg COD L^{-1} (200 mmol per kg VSS), which displayed a positive relationship with GLDA dosage. In addition, SL-EPS and LB-EPS together accounted for 26.1% of the total extracted EPS in the control, while it increased to 53.6% with 200 mmol per kg VSS GLDA supplemented. It indicated that more EPS became extractable and readily accessible for bacteria after the GLDA pretreatment, which is beneficial for the following fermentation process.

To further study the chemical structure changes, the organic compounds in the solid and liquid phases were characterized by FTIR and EEM fluorescence spectra, respectively. The FTIR spectra (Fig. 3b) show typical functional groups associated with polysaccharides and proteins (Table S3). Generally, the absorption peak at 3325 cm^{-1} might be caused by the tensile vibration of the O−H bond of the polysaccharides [39]. The characteristic vibration peak of carboxyl C=O (1655 cm^{-1}) in GLDA is the same as that of C=O in the amide I from the sludge [40]. However, the intensity of this peak gradually increased with increasing GLDA dosage, indicating that the C=O group in the chelating agent might contribute to this peak. In addition, the relationship between different functional groups in sludge samples pretreated with GLDA was verified by FTIR 2-COS maps [9]. As shown in Fig. 3c, the cross peaks of different functional groups (3325, 2930, 1655, 1530, 1425, and 1027 cm^{-1}) were all positive in the synchronous plot, indicating that the changes of those corresponding functional groups in the pretreated sludge samples were consistent. The combination of synchronous and asynchronous maps could further clarify the sequential relationship among functional groups [33]. As depicted (Fig. 3d), with GLDA dosage increasing, the functional group variation sequence follows: O−H stretching > C−OH and C−O−C stretching > C=O and C=N stretching > C−H stretching > stretching of carboxylic O−C−O vibration > N−H and C−N stretching. The results showed that O−H stretching, C−OH, and C−O−C stretching related to polysaccharides changed prior to C=O and C=N stretching (amide I) and N−H and C−N stretching (amide II) related to proteins. Therefore, the changes of the O−H, C−O, and C−O−C functional groups occurred first with GLDA pretreatment, and polysaccharide was the most affected by the increase of GLDA dosage.

Studies have shown that the secondary structure of protein has a strong impact on microbial aggregation and EPS structures [40]. When the α-helix content is low, and the β-sheet and random coil contents are high, the protein molecule has a loose structure and exposure to more hydrophobic sites inside the molecule [33]. The relative contents of different protein secondary structures are displayed in Table S4. The α-helix/(β-sheet + random coil) ratio of sludge pretreated with GLDA (0.51 in 200 mmol per kg VSS test) is significantly lower than the control (0.85). It indicated that GLDA pretreatment resulted in loose structure. The exposed hydrophobic sites might benefit bacteria to contact and utilize the organics in sludge. Considering that the hydrogen bond (about 2 kcal mol^{-1}) is the main force for maintaining secondary structure, it may also suggest that GLDA pretreatment could damage the hydrogen bond of sludge protein [9], which further reduces the energy barrier required for sludge hydrolysis.

The EEM fluorescence spectra of the supernatant are presented in Fig. 4. Two main peaks were observed at an Ex/Em of 200−240
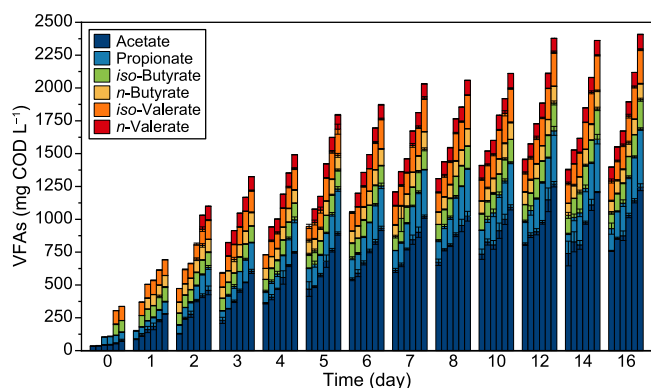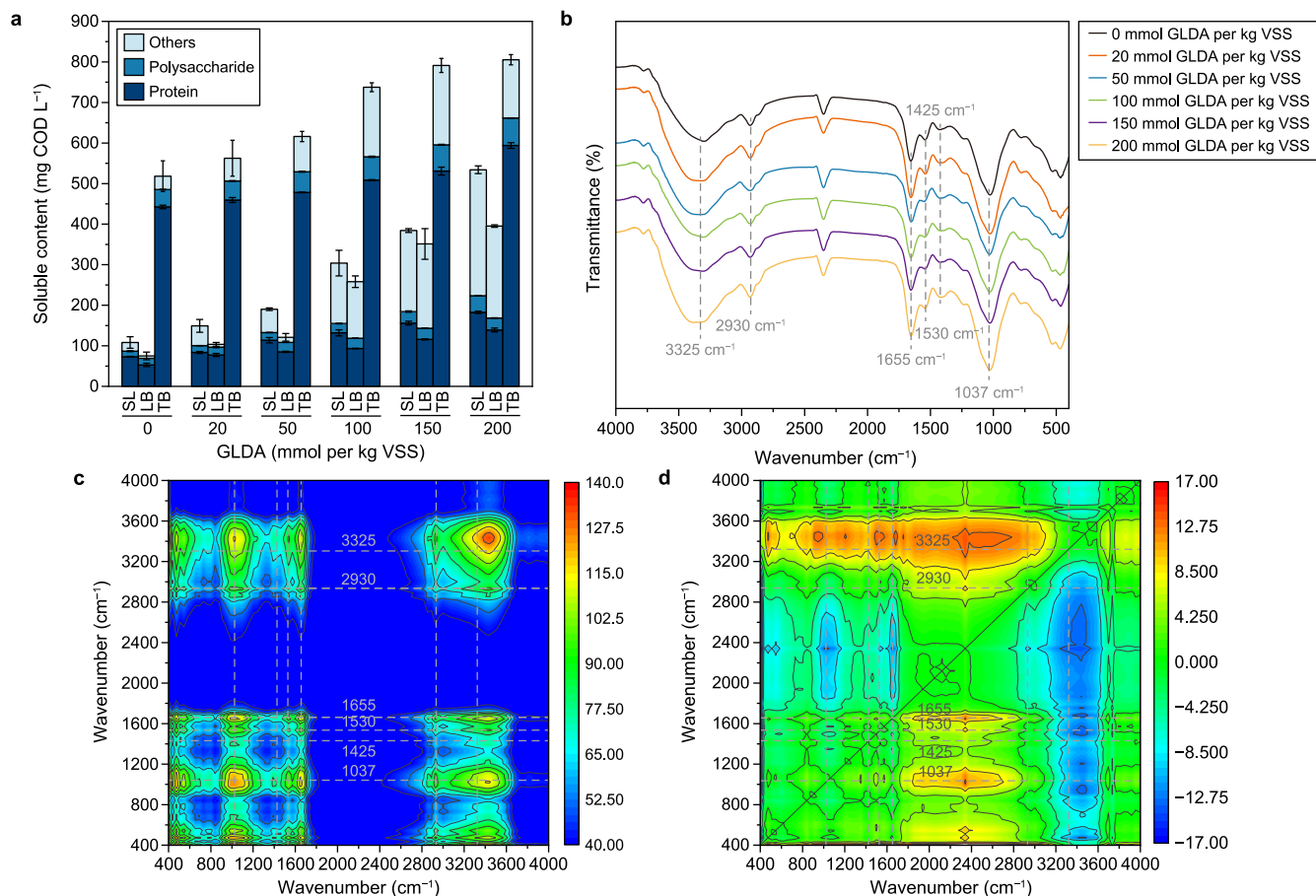
Fig. 3. a, Variations of polysaccharide and protein within SL-, LB- and TB-EPS of sludges pretreated by different GLDA dosages. **b,** FTIR spectra of different sludge samples after the pretreatment. **c–d,** Synchronous (**c**) and asynchronous (**d**) 2D-COS map of sludge after pretreatment.

nm/320−390 nm (peak A) and 260−280 nm/320−390 nm (peak B). Peaks A and B were attributed to aromatic protein and soluble microbial byproduct-like organics (such as tryptophan protein), respectively [41]. Those protein-like organic matters were supposed to be readily used by the fermentation bacteria. The fluorescence intensities of both peaks increased with higher GLDA dosages, indicating that the pretreatment improved the solubilization of organic matters from WAS solid phase, which was

Fig. 4. EEM fluorescence spectra of sludge supernatant corresponding to GLDA dosages of 0 (**a**), 20 (**b**), 50 (**c**), 100 (**d**), 150 (**e**), and 200 (**f**) mmol per kg VSS.

consistent with the increased SL-EPS content as discussed previously (Fig. 3a). Fluorescence regional integration (FRI) analysis was further conducted. The distribution of different regions is shown in Fig. S3. Microbial byproduct and protein-like organics (region I, II, and IV) together accounted for around 80% of the total fluorescence intensity. The integrated fluorescence intensity of those areas was also reported to take the dominant place in previous studies [39,42]. Among them, microbial byproduct-like organics (region IV) increased from 18.8% to 29.5%, positively related to GLDA dosage. Humic acid-like organics (region V) remained almost still around 6%, while fulvic acid-like organics (region III) abundance decreased slightly from 14.2% to 9.7%. It implied that GLDA mainly targeted proteins in the EPS rather than humic substances.

Thermodynamics was further analyzed to gain more knowledge on the enhanced WAS solubilization by GLDA pretreatment based on the TOC solubilization performances (Fig. S4). The k value at 60 °C (solubilization rate constant) of pretreated sludge increased to 0.01375 min^{-1} compared to the control (0.01099 min^{-1}), implying that the pretreatment did facilitate the organic solubilization rate from sludge (Table S5). Furthermore, the AAE of sludge solubilization (control and 100 mmol per kg VSS tests) was calculated based on the Arrhenius equation (Text S2). The AAE value was reduced to 10.6 from 20.0 kJ mol^{-1} (control) after the pretreatment (Fig. S5d). The AAE reduction rate (47%) was similar to the previous study (49%) with isoelectric point pretreatment [43]. This reduction confirmed that the energy barrier of the WAS solubilization was lowered, and the organic solubilization potential of sludge was
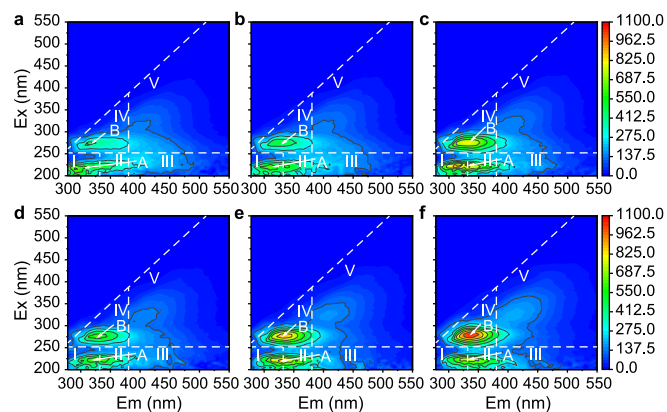
therefore improved by GLDA. According to these results, it can be concluded that the GLDA pretreatment could facilitate the organic solubilization rate and improve the organic solubilization potential of sludge.

3.3. Physical property and morphology variation

The study investigated the effect of the GLDA pretreatment on the physical characteristics of WAS. The thermos-stability of the WAS flocs was determined by thermogravimetric (TG) and derivative thermogravimetric (DTG) curves (Fig. S5), and no obvious variations in sludge thermos-stability were observed. The initial weight loss in WAS is attributed to moisture evaporation, including cellular and external bound water. Further weight reduction within the range of 240−600 °C can be attributed to destroying the organic fractions of sludge, such as proteins, polysaccharides, lipids, and humic acids [9]. This indicated that the pretreatment imposed little effect on the thermos-stability of the WAS flocs. As shown in Fig. 5, the zeta potential gradually decreased with higher GLDA. The zeta potential of the control sample was −16.1 mV, while that of the 200 mmol per kg VSS sample decreased to about −20.7 mV. This suggests that the GLDA increased negative charges of the sludge flocs. The electrostatic repulsion between sludge flocs was supposed to be enhanced, which was detrimental to sludge flocculation [44]. The CST of the control was about 28.4 s, which increased to 65.4 s after pretreatment with 200 mmol per kg VSS GLDA. Hence, it indicated that the dewaterability deteriorated significantly with GLDA, as observed in other pretreatment studies [36,45]. The deteriorated dewatering property might be caused by solid organic matter solubilization and the resulting viscosity increase [41]. It might further imply that GLDA induced solubilization of WAS flocs.

The WAS morphology and component distribution after pretreatment with different concentrations of GLDA were directly imaged with CLSM. As shown in Fig. 6, the cells, α-D-glucopyranose, β-D-glucopyranose, and proteins were distributed evenly within the WAS flocs, indicating that the bacteria cells were covered with proteins and polysaccharides (i.e., EPS), which was also observed by previous study [9]. In addition, it was found that the control sludge flocs were more aggregated and denser, while they showed a clear tendency to be looser and sparser with increasing GLDA dosages. It demonstrated that GLDA released organic matters from the solid phase of WAS, which follows the observed EPS structure (Fig. 3a). Smaller sludge particles and lower dewaterability are always related to a higher specific surface area [46], which can provide a better contract between the substrate and the anaerobic bacteria.
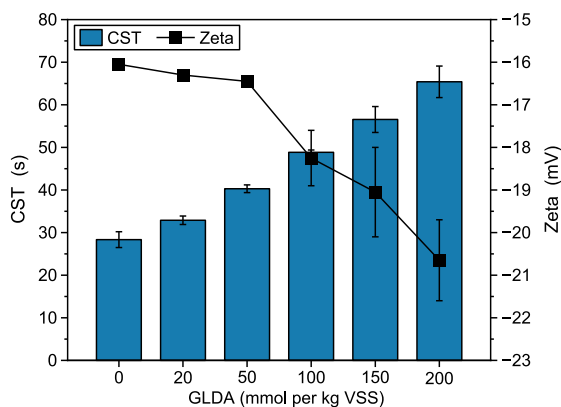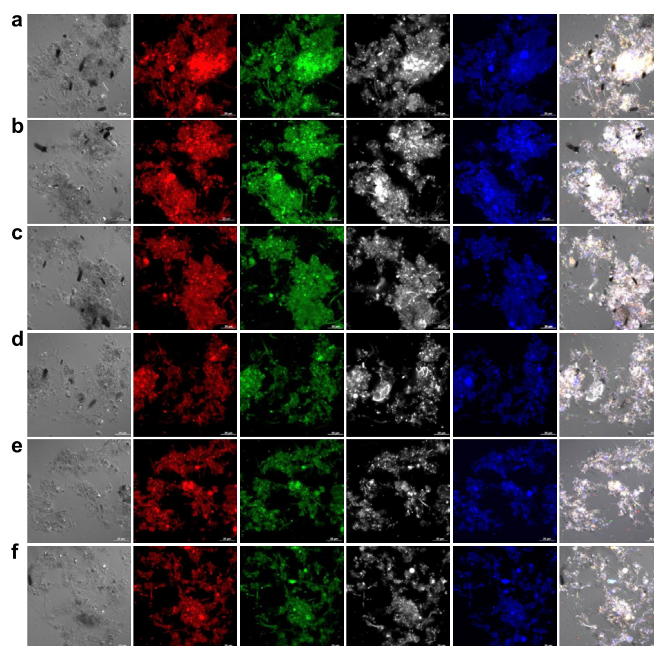

Fig. 6. CLSM images of pretreated sludge corresponding to GLDA dosages of 0 (**a**), 20 (**b**), 50 (**c**), 100 (**d**), 150 (**e**), and 200 (**f**) mmol per kg VSS. From left to right are bright fields, nucleic acid (SYTO 63), α-D-glucopyranose (Con A), β-D- glucopyranose (CW), protein (FITC), and merged images. Scale bar = 20 μm.

Therefore, the loose and sparse flocs are expected to be more readily utilized by bacteria for VFAs production.

3.4. Speciation of representative multivalent metals

GLDA is a chelating agent expected to target the metal ions within the WAS flocs [22]. Hence, the effects of GLDA on representative multivalent metals Fe, Ca, and Mg were investigated (Fig. 7). The concentrations of all three metals increased in the supernatant with the increasing GLDA level. Among them, Ca and Fe ions were the main metals released, as observed in other studies with EDTA and isoelectric point pretreatments [8,43]. In detail, the concentration of soluble Ca increased from 32.3 to 101.4 mg L^{-1}, showing an increasement of 215%. Similarly, the Fe concentration increased from 1.0 to 110.8 mg L^{-1}, suggesting that Fe was most distributed in the solid phase. However, the Mg ion only increased from 5.2 to 13.1 mg L^{-1} during the same process. To further explore metal release from WAS solids, the speciation distribution of the above metals was also determined. It could be observed that most of the exchangeable and organic-binding Fe were released from the solid phase. Similarly, the organic-binding Ca was the main speciation released by GLDA. This observation is consistent with previous studies, which noted that Ca and Fe in exchangeable and organic-binding forms were more easily extracted during EPS layer delamination [9]. However, the speciation distribution of Mg in the WAS solids remained relatively still during the pretreatment. SEM-EDS also supported that the Fe abundance in the solids decreased significantly after the pretreatment, while Mg increased simultaneously (Table S6).

The GLDA pretreatment removed multivalent metals, potentially exposing more negatively charged functional groups on the sludge surface. It could also explain the lower zeta potential after pretreatment. Furthermore, the multivalent metal-binding functional groups, such as phosphoryl, carboxyl, sulfhydryl, and hydroxyl, were always regarded as the enzyme binding sites [15].

Fig. 5. CST and zeta potential of different samples after GLDA pretreatment. The error bar represented the standard error of triplicates.
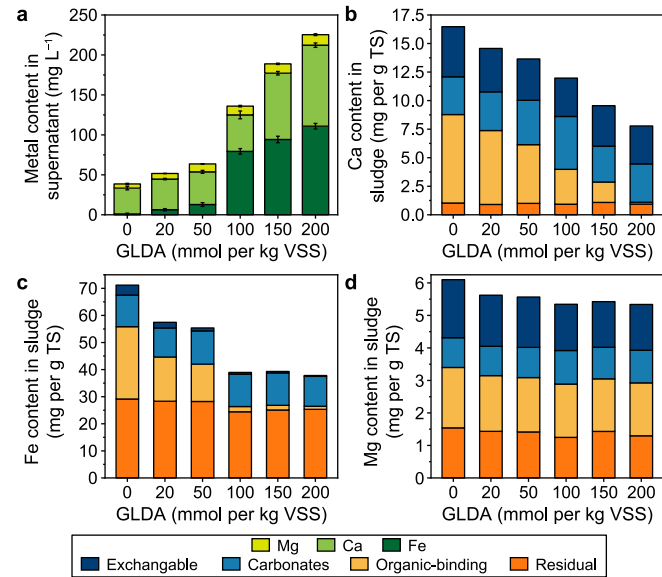
Fig. 7. a, Soluble metals released in the supernatant after pretreatment with different GLDA dosages. **b**−**d**, Metal distribution in different fractions in sludge solids after pretreatment: Mg (**b**), Ca (**c**), and Fe (**d**).
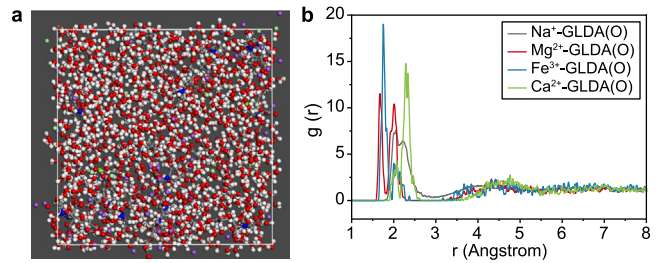

Fig. 8. Interaction between GLDA functional group (-OH) and metal ions: Trajectories (**a**) and RDF (**b**).

Moreover, the diffusion coefficients of these four cations, obtained by mean-square deviation (MSD), were $1.45 \times 10^{-5}\,\text{cm}^2\,\text{s}^{-1}\,(\text{Ca}^{2+}) > 1.02 \times 10^{-5}\,\text{cm}^2\,\text{s}^{-1}\,(\text{Na}^+) > 0.79 \times 10^{-5}\,\text{cm}^2\,\text{s}^{-1}\,(\text{Mg}^{2+}) > 0.29 \times 10^{-5}\,\text{cm}^2\,\text{s}^{-1}\,(\text{Fe}^{3+})$. This trend further suggested that the interconnected interaction between Fe^{3+} and GLDA may be an important factor limiting carbon release.

3.5. Effect of GLDA on microbial community

The microbial community was characterized to explore community shifts induced by the pretreatment (Table S7). The Coverage indexes were around 0.99 for all the samples, implying that most of the bacteria were detected. However, no significant variations in these indices were observed with different GLDA dosages, indicating that the pretreatment only slightly impacted the community diversity. The GLDA is reported to be completely degraded into CO_2 and ammonium by some bacteria, which could explain the little effect it imposes on the microbial community [48]. The Venn diagram and microbial distribution (Fig. S8) also indicated that GLDA negatively affected microbial communities with different GLDA dosages. Over 900 OTUs (operational taxonomic units) were shared among those samples (over 80% OTUs of each sample). It indicated that the microbial community and function were not obviously disturbed in the presence of GLDA. The bacterial distribution at the phylum level indicated that all of the samples were dominated by phylum Chloroflexi, Proteobacteria, Actinobacteriota, Bacteroidota, and Firmicutes, which are also widely found in other VFAs production systems [36,49]. The abundance of phylum Chloroflexi decreased slightly, while that of phylum Proteobacteria, Actinobacteria, and Firmicutes slightly increased with higher GLDA dosages. Bacteria from Proteobacteria, Actinobacteria, and Firmicutes were reported to be able to degrade complex organic matter or produce VFAs [50]. Considering that anaerobic fermentation is a biological process, those results implied that GLDA imposed minimal effect on the reactor stability, making it a perfect pretreatment agent without worrying about any significant disturbance it might bring about.

3.6. Economic analysis

The study also analyzed the economic feasibility of the VFAs production system from GLDA pretreated WAS (Table S8). The

Hence, the increased number of enzyme binding sites resulting from GLDA pretreatment would lead to enhanced solubilization or hydrolysis of WAS flocs. To analyze the species distribution and interactions between the functional group of GLDA and metal cations (i.e., Mg^{2+}, Fe^{3+}, and Ca^{2+}), XPS analysis was conducted (Fig. S7). The two main peaks in the XPS spectra correspond to oxygen and carbon at around 533 and 285 eV, respectively. Additionally, three Ca 2p, Fe, 2p, and Mg 1s peaks were detected at 346.41, 710.43, and 1302.71 eV, respectively [47]. Under different dosages of GLDA, Ca 2p and Mg 1s did not experience any noticeable changes. However, the atomic percentage of Fe increased from 3.99% to 4.62% and then slightly declined to 3.39% (Table 2). The differences in atomic percentages of different cations could be due to the different interactions, such as Ca^{2+} and Mg^{2+} being adsorbed to GLDA through ion exchange, while Fe^{3+} was adsorbed through ion exchange and complexation.

To further investigate the interactions between GLDA and metal cations, an MD simulation was conducted at a 20% GLDA condition. After simulations at constant volume and temperature (NVT), and constant pressure and temperature (NPT), the system reached a relaxed state (Fig. 8a), and the sequence data was collected with constant volume and energy (NVE). The RDF (Radial Distribution Functions) values of GLDA(O) and cations (Na^+, Mg^{2+}, Fe^{3+}, and Ca^{2+}) are shown in Fig. 8b. The order of RDF value was $\text{Fe}^{3+} > \text{Ca}^{2+} > \text{Mg}^{2+} > \text{Na}^+$, indicating that Fe^{3+} had the highest probability of finding a particle at a distance r from GLDA tagged particle, while Na^+ has the lowest probability. This observation was consistent with the fact that more Fe and Ca were released than Mg.

Table 2
Binding energy and atomic percentage under different GLDA dosages (mmol per kg VSS).

Elements	0		20		50		100		150		200	
	BE (eV)	Ato (%)	BE (eV)	Ato (%)	BE (eV)	Ato (%)	BE (eV)	Ato (%)	BE (eV)	Ato (%)	BE (eV)	Ato (%)
C 1s	284.10	93.20	284.76	92.32	284.72	92.64	285.93	93.60	285.50	93.66	284.78	93.92
Ca 2p	346.41	2.20	346.50	2.23	346.97	2.28	348.33	2.01	347.84	2.17	346.87	2.11
Fe 2p	710.43	3.99	710.96	4.62	710.96	4.23	712.17	3.69	711.76	3.47	711.01	3.39
Mg 1s	1302.71	0.60	1302.53	0.82	1303.56	0.85	1303.88	0.70	1304.05	0.70	1303.09	0.58

market price of industrial GLDA used for WAS pretreatment is about ¥7000 t^{-1} (40%). Taking the experimental test with the highest VFAs production as an example (200 mmol GLDA per kg VSS test and the VFAs yield is 241.03 mg COD per g VSS), the input cost of GLDA was ¥5.5 $\times$ 10^{-4} per g TSS after calculation. Based on the market prices of VFAs products (acetic acid: ¥6200 t^{-1}, propionic acid: ¥11700 t^{-1}, *n*-butyric acid: ¥14500 t^{-1}, *iso*-butyric acid: ¥16000 t^{-1}, *n*-valeric acid: ¥27000 t^{-1}, *iso*-valeric acid: ¥36000 t^{-1}), the profit value is calculated from the amount of individual VFA produced (Fig. 2). The potential net profit of GLDA-WAS fermentation was then calculated as positive. Compared with other WAS pretreatment methods, GLDA pretreatment has significantly higher net profits than K_2FeO_4 [51], biosurfactant + microwave [52], CaO_2 + thermal [53], NaOH + ultrasound [54], and K_2FeO_4/$NaNO_2$ pretreatment, while slightly lower than $NaNO_2$ [51] and nitrous acid + freezing pretreatment [55]. Given the advantages of GLDA pretreatment in operation simplicity, high biodegradability, and low toxicity to organisms, it has broad application prospects in WAS pretreatment to improve the anaerobic VFAs production efficiency and the potential profit return.

4. Conclusions

This study demonstrated the effect of GLDA pretreatment on WAS and VFAs production during anaerobic fermentation. The total VFAs production from WAS increased by 64% after this pretreatment (200 mmol per kg VSS GLDA), with acetate as the most dominant product. Only a few organic matters (less than 600 mg COD L^{-1}) were dissolved directly by GLDA from the WAS solids. Instead, the primary effect of this pretreatment was to induce a looser structural configuration and higher extractability of EPS, which was supported by the morphology and lower solubilization energy barrier (reduced to 10.6 from 20 kJ mol^{-1}) for WAS flocs. The GLDA was observed to target the organic-binding metal ions. Over 95% of the Fe and Ca in this form were released into the liquid phase, while extraction of Mg was minimal. The MD calculation confirmed that GLDA has a higher affinity to Fe^{3+} and Ca^{2+} than Mg^{2+}. Moreover, GLDA is relatively friendly to bacteria and displayed satisfactory economic feasibility compared to other pretreatment methods. The findings of this study highlight the potential of GLDA pretreatment as a promising approach for enhancing anaerobic VFAs production from WAS.

CRediT authorship contribution statement

Chang Liu: Conceptualization, Methodology, Investigation, Formal Analysis, Writing - Original Draft. **Lin Li**: Conceptualization, Funding Acquisition, Supervision, Validation, Writing - Review & Editing. **Linji Xu**: Methodology, Formal Analysis. **Tanglong Zhang**: Investigation, Data Curation. **Qiang He**: Funding Acquisition, Supervision, Writing - Review & Editing. **Xiaodong Xin**: Formal Analysis, Writing - Review & Editing.

Declaration of competing interest

The authors declare that they have no known competing financial interests or personal relationships that could have appeared to influence the work reported in this paper.

Acknowledgements

Appendix A. Supplementary data

Supplementary data to this article can be found online at https://doi.org/10.1016/j.ese.2024.100393.

References

[1] Y. Xu, Y.Q. Lu, L.K. Zheng, Z.W. Wang, X.H. Dai, Perspective on enhancing the anaerobic digestion of waste activated sludge, J. Hazard Mater. 389 (2020) 16.

[2] L.Y. Feng, J.Y. Luo, Y.G. Chen, Dilemma of sewage sludge treatment and disposal in China, Environ. Sci. Technol. 49 (2015) 4781−4782.

[3] T. Mahmood, A. Elliott, A review of secondary sludge reduction technologies for the pulp and paper industry, Water Res. 40 (2006) 2093−2112.

[4] Q. Fu, D.B. Wang, X.M. Li, Q. Yang, Q.X. Xu, B.J. Ni, Q.L. Wang, X.R. Liu, Towards hydrogen production from waste activated sludge: principles, challenges and perspectives, Renew. Sustain. Energy Rev. 135 (2021) 12.

[5] H. Yang, J.Y. Liu, P.S. Hu, L.P. Zou, Y.Y. Li, Carbon source and phosphorus recovery from iron-enhanced primary sludge via anaerobic fermentation and sulfate reduction: performance and future application, Bioresour. Technol. 294 (2019) 9.

[6] S.L. Wu, J. Sun, X.M. Chen, W. Wei, L. Song, X.H. Dai, B.J. Ni, Unveiling the mechanisms of medium-chain fatty acid production from waste activated sludge alkaline fermentation liquor through physiological, thermodynamic and metagenomic investigations, Water Res. 169 (2020) 12.

[7] L. Li, J.G. He, X.D. Xin, M.F. Wang, J. Xu, J. Zhang, Enhanced bioproduction of short-chain fatty acids from waste activated sludge by potassium ferrate pretreatment, Chem. Eng. J. 332 (2018) 456−463.

[8] Y. Xu, Y.Q. Lu, X.H. Dai, B. Dong, The influence of organic-binding metals on the biogas conversion of sewage sludge, Water Res. 126 (2017) 329−341.

[9] S.Q. Li, Y. Zhang, W.D. Duan, R. Deng, L. Gu, D.Z. Shi, Insights into the resistance of different extracellular polymeric substance (EPS) layers to the fermentation environment in sludge anaerobic digestion, Chem. Eng. J. 449 (2022) 12.

[10] H.S. Li, Y. Wen, A.S. Cao, J.S. Huang, Q. Zhou, P. Somasundaran, The influence of additives (Ca2+, Al3+, and Fe3+) on the interaction energy and loosely bound extracellular polymeric substances (EPS) of activated sludge and their flocculation mechanisms, Bioresour. Technol. 114 (2012) 188−194.

[11] H.C. Flemming, J. Wingender, The biofilm matrix, Nat. Rev. Microbiol. 8 (2010) 623−633.

[12] A.F.M. Braga, M. Zaiat, G.H.R. Silva, F.G. Fermoso, Metal fractionation in sludge from sewage UASB treatment, J. Environ. Manag. 193 (2017) 98−107.

[13] F. Suanon, Q. Sun, D. Mama, J.W. Li, B. Dimon, C.P. Yu, Effect of nanoscale zerovalent iron and magnetite (Fe3O4) on the fate of metals during anaerobic digestion of sludge, Water Res. 88 (2016) 897−903.

[14] Y. Xu, H. Geng, R.J. Chen, R. Liu, X.H. Dai, Enhancing methanogenic fermentation of waste activated sludge via isoelectric-point pretreatment: insights from interfacial thermodynamics, electron transfer and microbial community, Water Res. 197 (2021) 14.

[15] Y. Xu, L.K. Zheng, H. Geng, R. Liu, X.H. Dai, Enhancing acidogenic fermentation of waste activated sludge via isoelectric-point pretreatment: insights from physical structure and interfacial thermodynamics, Water Res. 185 (2020) 11.

[16] H.B. Liu, H. Xiao, B. Yin, Y.P. Zu, H. Liu, B. Fu, H.J. Ma, Enhanced volatile fatty acid production by a modified biological pretreatment in anaerobic fermentation of waste activated sludge, Chem. Eng. J. 284 (2016) 194−201.

[17] A. Vintiloiu, M. Boxriker, A. Lemmer, H. Oechsner, T. Jungbluth, E. Mathies, D. Ramhold, Effect of ethylenediaminetetraacetic acid (EDTA) on the bioavailability of trace elements during anaerobic digestion, Chem. Eng. J. 223 (2013) 436−441.

[18] C.E. Noradoun, I.F. Cheng, EDTA degradation induced by oxygen activation in a zerovalent iron/air/water system, Environ. Sci. Technol. 39 (2005) 7158−7163.

[19] E. Meers, A. Ruttens, M.J. Hopgood, D. Samson, F.M.G. Tack, Comparison of EDTA and EDDS as potential soil amendments for enhanced phytoextraction of heavy metals, Chemosphere 58 (2005) 1011−1022.

[20] G.Y. Wang, S.R. Zhang, X.X. Xu, Q.M. Zhong, C.E. Zhang, Y.X. Jia, T. Li, O.P. Deng, Y. Li, Heavy metal removal by GLDA washing: optimization, redistribution, recycling, and changes in soil fertility, Sci. Total Environ. 569 (2016) 557−568.

[21] Q. Wu, Y.R. Cui, Q.L. Li, J.H. Sun, Effective removal of heavy metals from industrial sludge with the aid of a biodegradable chelating ligand GLDA, J. Hazard Mater. 283 (2015) 748−754.

[22] D. Kolodynska, Cu(II), Zn(II), Co(II) and Pb(II) removal in the presence of the complexing agent of a new generation, Desalination 267 (2011) 175−183.

[23] N.R. Itrich, K.M. McDonough, C.G. van Ginkel, E.C. Bisinger, J.N. LePage, E.C. Schaefer, J.Z. Menzies, K.D. Casteel, T.W. Federle, Widespread microbial adaptation to L-glutamate-N,N-diacetate (L-GLDA) following its market

introduction in a consumer cleaning product, Environ. Sci. Technol. 49 (2015) 13314—13321.

[24] N.V. Thinh, Y. Osanai, T. Adachi, B.T.S. Vuong, I. Kitano, N.T. Chung, P.K. Thai, Removal of lead and other toxic metals in heavily contaminated soil using biodegradable chelators: GLDA, citric acid and ascorbic acid, Chemosphere 263 (2021) 12.

[25] H. Geng, Y. Xu, L.K. Zheng, H. Gong, L.L. Dai, X.H. Dai, An overview of removing heavy metals from sewage sludge: achievements and perspectives, Environ. Pollut. 266 (2020) 15.

[26] K. Dai, T. Sun, Y. Yan, D.K. Qian, W. Zhang, F. Zhang, R.J.X. Zeng, Electricity production and microbial community in psychrophilic microbial fuel cells at 10 degrees C, Bioresour, Technol. 313 (2020) 8.

[27] J.Q. Wang, M. Yang, R.P. Liu, C.Z. Hu, H.J. Liu, J.H. Qu, Anaerobically-digested sludge conditioning by activated peroxymonosulfate: significance of EDTA chelated-Fe2+, Water Res. 160 (2019) 454—465.

[28] W. Chen, P. Westerhoff, J.A. Leenheer, K. Booksh, Fluorescence excitation - emission matrix regional integration to quantify spectra for dissolved organic matter, Environ. Sci. Technol. 37 (2003) 5701—5710.

[29] H. Xu, Y. Xu, L.K. Zheng, H.Y. Liu, X.H. Dai, Cation exchange resin pre-treatment enhancing methane production from anaerobic digestion of waste activated sludge, Water Res. 212 (2022) 13.

[30] A.P.H.A. APHA, Standard Methods for Examination of Water and Wastewater, twenty-first ed., 2005. Washington, DC.

[31] X.R. Liu, Y.X. Wu, Q.X. Xu, M.T. Du, D.B. Wang, Q. Yang, G.J. Yang, H. Chen, T.J. Zeng, Y.W. Liu, Q.L. Wang, B.J. Ni, Mechanistic insights into the effect of poly ferric sulfate on anaerobic digestion of waste activated sludge, Water Res. 189 (2021) 12.

[32] F. Huang, H.B. Liu, J.X. Wen, C. Zhao, L. Dong, H. Liu, Underestimated humic acids release and influence on anaerobic digestion during sludge thermal hydrolysis, Water Res. 201 (2021) 13.

[33] S.N. Peng, Z.Y. Wang, P.F. Yu, G.Y. Liao, R. Liu, D.S. Wang, W.J. Zhang, Aggre-gation and construction mechanisms of microbial extracellular polymeric substances with the presence of different multivalent cations: molecular dynamic simulation and experimental verification, Water Res. 232 (2023) 9.

[34] Y.C. She, W.X. Wei, X.H. Ai, J.M. Hong, X.D. Xin, Synergistic pretreatment of CaO and freezing/thawing to enhance volatile fatty acids recycling and dewaterability of waste activated sludge via anaerobic fermentation, Che-mosphere 280 (2021) 10.

[35] D.B. Wang, Y.X. Huang, Q.X. Xu, X.R. Liu, Q. Yang, X.M. Li, Free ammonia aids ultrasound pretreatment to enhance short-chain fatty acids production from waste activated sludge, Bioresour. Technol. 275 (2019) 163—171.

[36] J.Q. Xie, X.D. Xin, X.H. Ai, J.M. Hong, Z.D. Wen, W. Li, S.H. Lv, Synergic role of ferrate and nitrite for triggering waste activated sludge solubilisation and acidogenic fermentation: effectiveness evaluation and mechanism elucida-tion, Water Res. 226 (2022) 15.

[37] X.L. Liu, A.J. Li, L.S. Ma, Z.T. Jing, J. Yang, Y. Tang, B. Hu, A comparison on phosphorus release and struvite recovery from waste activated sludge by different treatment methods, Int. Biodeterior. Biodegrad. 148 (2020) 8.

[38] S. Felz, P. Vermeulen, M.C.M. van Loosdrecht, Y.M. Lin, Chemical character-ization methods for the analysis of structural extracellular polymeric sub-stances (EPS), Water Res. 157 (2019) 201—208.

[39] H.X. Guo, S. Felz, Y.M. Lin, J.B. van Lier, M. de Kreuk, Structural extracellular polymeric substances determine the difference in digestibility between waste activated sludge and aerobic granules, Water Res. 181 (2020) 10.

[40] F.X. Jia, Q. Yang, X.H. Liu, X.Y. Li, B.K. Li, L. Zhang, Y.Z. Peng, Stratification of extracellular polymeric substances (EPS) for aggregated anammox

microorganisms, Environ. Sci. Technol. 51 (2017) 3260—3268.

[41] H.Y. He, X.D. Xin, W. Qiu, D. Li, Z.C. Liu, J. Ma, Role of nano-Fe3O4 particle on improving membrane bioreactor (MBR) performance: alleviating membrane fouling and microbial mechanism, Water Res. 209 (2022) 10.

[42] L. Guo, M.M. Lu, Q.Q. Li, J.W. Zhang, Y. Zong, Z.L. She, Three-dimensional fluorescence excitation-emission matrix (EEM) spectroscopy with regional integration analysis for assessing waste sludge hydrolysis treated with multi-enzyme and thermophilic bacteria, Bioresour. Technol. 171 (2014) 22—28.

[43] Y. Xu, Y.Q. Lu, X.H. Dai, L.L. Dai, Enhancing anaerobic digestion of waste activated sludge by solid-liquid separation via isoelectric point pretreatment, ACS Sustain. Chem. Eng. 6 (2018) 14774—14784.

[44] Q. Liu, Y.F. Li, F. Yang, X.R. Liu, D.B. Wang, Q.X. Xu, Y. Zhang, Q. Yang, Un-derstanding the mechanism of how anaerobic fermentation deteriorates sludge dewaterability, Chem. Eng. J. 404 (2021) 9.

[45] Y.F. Li, X.Z. Yuan, Z.B. Wu, H. Wang, Z.H. Xiao, Y. Wu, X.H. Chen, G.M. Zeng, Enhancing the sludge dewaterability by electrolysis/electrocoagulation com-bined with zero-valent iron activated persulfate process, Chem. Eng. J. 303 (2016) 636—645.

[46] W.B. Yu, J.K. Yang, Y.F. Shi, J. Song, Y. Shi, J. Xiao, C. Li, X.Y. Xu, S. He, S. Liang, X. Wu, J.P. Hu, Roles of iron species and pH optimization on sewage sludge conditioning with Fenton's reagent and lime, Water Res. 95 (2016) 124—133.

[47] C.T. Zhu, I. Dobryden, J. Ryden, S. Oberg, A. Holmgren, A.P. Mathew, Adsorp-tion behavior of cellulose and its derivatives toward Ag(I) in aqueous me-dium: an AFM, spectroscopic, and DFT study, Langmuir 31 (2015) 12390—12400.

[48] C.G. van Ginkel, R. Geerts, P.D. Nguyen, C.M. Plugge, Biodegradation pathway of L-glutamatediacetate by *Rhizobium radiobacter* strain BG-1, Int. Biodeterior. Biodegrad. 62 (2008) 31—37.

[49] C.X. Yang, A.J. Zhou, Z.W. He, L. Jiang, Z.C. Guo, A.J. Wang, W.Z. Liu, Effects of ultrasonic-assisted thermophilic bacteria pretreatment on hydrolysis, acidi-fication, and microbial communities in waste-activated sludge fermentation process, Environ. Sci. Pollut. Res. 22 (2015) 9100—9109.

[50] Q. Zhang, S.Y. Fang, X.S. Cheng, F. Wang, L. Zhang, W.X. Huang, W. Du, F. Fang, J.S. Cao, J.Y. Luo, Persulfate-based strategy for promoted acesulfame removal during sludge anaerobic fermentation: combined chemical and biological ef-fects, J. Hazard Mater. 434 (2022) 10.

[51] J. Xie, X. Xin, X. Ai, J. Hong, Z. Wen, W. Li, S. Lv, Synergic role of ferrate and nitrite for triggering waste activated sludge solubilisation and acidogenic fermentation: effectiveness evaluation and mechanism elucidation, Water Res. 226 (2022) 119287.

[52] J. Xiao, L. Zhao, Z. Shen, Enhanced sludge anaerobic fermentation using mi-crowave pretreatment combined with biosurfactant alkyl polyglycoside, RSC Adv. 7 (2017) 43772—43779.

[53] X.R. Liu, Q.X. Xu, D.B. Wang, Q. Yang, Y.X. Wu, J.N. Yang, Y.W. Liu, Q.L. Wang, B.J. Ni, X.M. Li, H.L. Li, G.J. Yang, Enhanced short-chain fatty acids from waste activated sludge by heat-CaO2 advanced thermal hydrolysis pretreatment: parameter optimization, mechanisms, and implications, ACS Sustain. Chem. Eng. 7 (2019) 3544—3555.

[54] Y. Yan, L. Feng, C. Zhang, C. Wisniewski, Q. Zhou, Ultrasonic enhancement of waste activated sludge hydrolysis and volatile fatty acids accumulation at pH 10.0, Water Res. 44 (2010) 3329—3336.

[55] Y. Wu, K. Song, X. Sun, H. Ngo, W. Guo, L.D. Nghiem, Q. Wang, Mechanisms of free nitrous acid and freezing co-pretreatment enhancing short-chain fatty acids production from waste activated sludge anaerobic fermentation, Che-mosphere 230 (2019) 536—543.